J. Fluid Mech. (2021), *vol*. 912, A33, doi:10.1017/jfm.2020.1126

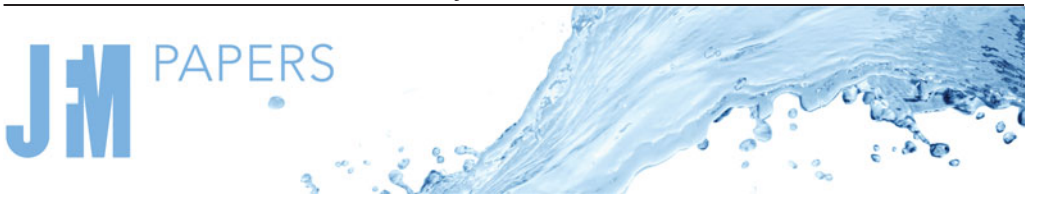

A velocity-variation-based formulation for bedload particle hops in rivers

Zi Wu[1,2,3,†], Arvind Singh[2], Efi Foufoula-Georgiou[3,4], Michele Guala[5], Xudong Fu[1] and Guangqian Wang[1]

[1]State Key Laboratory of Hydroscience and Engineering; Department of Hydraulic Engineering, Tsinghua University, Beijing 100084, PR China

[2]Department of Civil, Environmental and Construction Engineering, University of Central Florida, Orlando, FL 32816, USA

[3]Department of Civil and Environmental Engineering, University of California Irvine, Irvine, CA 92697, USA

[4]Department of Earth System Science, University of California Irvine, Irvine, CA 92697, USA

[5]St. Anthony Falls Laboratory, Department of Civil, Environmental and Geo-Engineering, University of Minnesota, Minneapolis, MN 55414, USA

(Received 3 July 2020; revised 31 October 2020; accepted 11 December 2020)

Bedload particle hops are defined as successive motions of a particle from start to stop, characterizing one of the most fundamental processes of bedload sediment transport in rivers. Although two transport regimes have been recently identified for short and long hops, respectively, there is still the lack of a theory explaining the mean hop distance–travel time scaling for particles performing short hops, which dominate the transport and may cover over 80 % of the total hop events. In this paper, we propose a velocity-variation-based formulation, the governing equation of which is intrinsically identical to that of Taylor dispersion for solute transport within shear flows. The key parameter, namely the diffusion coefficient, can be determined by hop distances and travel times, which are easier to measure and more accurate than particle accelerations. For the first time, we obtain an analytical solution for the mean hop distance–travel time relation valid for the entire range of travel times, which agrees well with the measured data. Regarding travel times, we identify three distinct regimes in terms of different scaling exponents: respectively, $\sim$1.5 for the initial regime and $\sim$5/3 for the transition regime, which define the short hops, and 1 for the Taylor dispersion regime defining long hops. The corresponding distribution of the hop distance is analytically obtained and experimentally verified. We also show that the conventionally used exponential distribution, as proposed by Einstein, is solely for long hops. Further validation of the present formulation is provided by comparing the simulated accelerations with measurements.

† Email addresses for correspondence: wuzi@tsinghua.edu.cn, wuzi@pku.edu.cn

Key words: sediment transport, mixing and dispersion

1. Introduction

Studying the transport of bedload sediment particles ranging from coarse sands to gravels can be a challenge due to complex fluid–particle and particle–particle interactions (Gonzalez *et al.* 2017). Depending on the temporal–spatial scale focused on, the underlying mechanisms dominating the bedload transport process can be very different. The pioneering work of Einstein (1937) considered the transport of bedload particles at a relatively large scale, which involves many entrainment and deposition events experienced by each single particle. He conceptualized this complex transport process as composed of fundamental elements of rests for static particles and hops (or steps) for moving particles. During rests, a particle can stay either on top of the riverbed or buried under the surface. The term 'hop' can be formally defined as the successive motions of a particle from the start to the end of its motion, or motions between a pair of adjacent entrainment and deposition events by the same particle. The random variable of hop distance (or step length) with its probability density function (p.d.f.) has since been extensively studied for probabilistic formulations of bedload sediment transport (Paintal 1971; Hassan, Church & Schick 1991; Parker, Paola & Leclair 2000; Ancey *et al.* 2008; Ancey 2010; Bradley & Tucker 2012; Hassan *et al.* 2013; Yager, Kenworthy & Monsalve 2015; Wilson 2018). For example, focusing on the exchange of bedload particles between those in motion and those staying in the riverbed, the streamwise transport of tracer particles has been intensively explored recently, with the aim of understanding the problem of anomalous diffusion. This progress has mostly involved the assumption of a thin-tailed p.d.f. of hop-distances during the implementation of theoretical (Ganti *et al.* 2010; Lajeunesse, Devauchelle & James 2018; Wu *et al.* 2019*a*,*b*), numerical (Fan *et al.* 2014, 2016; Pelosi *et al.* 2016) and experimental (Martin, Jerolmack & Schumer 2012; Bradley 2017; Liu, Pelosi & Guala 2019) approaches.

At the relatively small scale of bedload particle transport, especially focusing on particle hops, the motions of the entrained particles are complicated and can include rolling, sliding and saltating on top of the riverbed (Charru, Mouilleron & Eiff 2004; Lajeunesse, Malverti & Charru 2010; Roseberry, Schmeeckle & Furbish 2012; Seizilles *et al.* 2014; Fathel, Furbish & Schmeeckle 2015; Ballio *et al.* 2019; Hosseini-Sadabadi, Radice & Ballio 2019). To better characterize the hop distance as well as other kinematic quantities, detailed information regarding the motions of sediment particles during transport is required, which has led to several high-resolution bedload particle-tracking experiments in the past decade, capturing the trajectories of every moving particle (Charru *et al.* 2004; Lajeunesse *et al.* 2010; Martin *et al.* 2012; Roseberry *et al.* 2012; Ancey & Heyman 2014; Seizilles *et al.* 2014; Campagnol *et al.* 2015; Liu *et al.* 2019). The probability distributions for various kinematic quantities were then obtained empirically, including those of velocities, accelerations, hop distances, and travel times (time spent during a hop, denoted as τ in this paper). These results are key for understanding the underlying physics of hop processes, as well as assisting in theoretical formulations and numerical simulation, and serving as additional means of validation for the modelling of bedload sediment transport (Ancey & Heyman 2014; Fan *et al.* 2014).

Based on numerical simulations and experimental measurements, Wu, Furbish & Foufoula-Georgiou (2020) identified two distinct transport regimes for short and long hops, the mean hop distances (L_h) of which scale with their travel times (τ) quadratically

($L_h \sim \tau^2$) and linearly ($L_h \sim \tau$), respectively. This observation was critical to unify disparate views on particle velocity statistics (exponential versus Gaussian) reported in the literature, demonstrating that long hops alone contribute to the Gaussian type of particle velocity p.d.f., while a mixture of both short and long hops leads to the exponential distribution, commonly observed at low transport rates. Under the well-accepted assumption of an exponential travel-time distribution (Lajeunesse *et al.* 2010; Martin *et al.* 2012; Fathel *et al.* 2015; Liu *et al.* 2019), the linear scaling relation for long hops was linked to the empirical evidence of thin-tailed hop-distance distribution. However, since the governing equation can only be solved numerically, no analytical arguments were made to provide a theoretical basis for such scaling regimes in the mean hop distance–travel time relation (L_h–τ) (Wu *et al.* 2020). Consequently, a previous formulation of a mean-reverting process (Ancey & Heyman 2014) was resorted to in order to understand the motion of the long-hop particles (Wu *et al.* 2020). For short hops, however, which may cover over 80 % of the overall hops, there is still the lack of a theory that explains the hop distance–travel time scaling, leading to ambiguity in the scaling exponent reported in the literature (Roseberry *et al.* 2012; Fathel *et al.* 2015; Wu *et al.* 2020). Given the statistical persistence of short hops, such information is deemed critical for correctly estimating sediment transport rate.

Regarding the governing equation for bedload particle motions adopted by Wu *et al.* (2020), some unknown functions must first be determined before numerical simulations can be performed for particle hops. This is, however, not trivial, and requires high-precision measurements of particle motions enabling the correct estimate of Lagrangian or total acceleration. For example, acceleration estimates from the second derivative of particle positions require an order-of-magnitude higher frequency (250 frames per second) in video capturing (Roseberry *et al.* 2012; Liu *et al.* 2019), as compared to that in similar studies focusing on particle hop distances and waiting times (Martin *et al.* 2012). Data acquisition on particles' travel times and hop distances is thus less experimentally demanding: those data are easier to obtain (require much lower sampling frequency), more accurate and more likely to be statistically converged given that measurement duration is typically inversely related to the acquisition frame rate. We expect that a theoretical model that can be parametrized with such data would be more reliable and feasible to apply.

In this paper we mainly aim at theoretically analysing the relation between mean hop distances and travel times (L_h–τ relationship) during bedload particle hops, which provides insights into the shift of scaling regimes as observed by the numerical and experimental investigation of Wu *et al.* (2020). To achieve such a goal, we will characterize the velocity variations during bedload particle hops, embedding the information of accelerations into the derived governing equation. However, we emphasize that we do not attempt a physical interpretation of the velocity variations. The main novelties of the paper are the following. First, we propose a nonlinear transformation of the particle velocity resulting in a velocity difference $\Delta\zeta$ that can be approximated by a Gaussian random walk process and leads to the governing equation for particle hops (§ 2). Second, we show that the deduced governing equation is intrinsically identical to that describing a Taylor dispersion process for solute transport in shear flows (Taylor 1953; Wu & Chen 2014). Borrowing the analytical technique of concentration moments (Aris 1956) employed to study Taylor dispersion, we derive analytical solutions of the p.d.f.s of particles' travel times and hop distances, and a relation between the mean hop distances and the travel times valid across the whole range of scales involved, both excellently supported by experimental

data (Fathel *et al.* 2015). We then show that the estimation of the required parameters (e.g. the diffusion coefficient) in the particle motion governing equation can be made based on measurements of hop distances and travel times, with no need for the acceleration data. As a further validation, we confirm that the acceleration distribution obtained from numerical simulations of the proposed particle motion governing equation is consistent with that obtained from experimental measurements (§ 3). Finally, concluding remarks are provided in § 4.

2. Formulation

In this paper we analyse the one-dimensional (streamwise) transport of bedload sediment particles, which are of uniform size and in equilibrium transport conditions. This idealized theoretical set-up is in accordance with recent studies (Lajeunesse *et al.* 2010; Roseberry *et al.* 2012; Fathel *et al.* 2015) on the statistics of particle motions, specifically focusing on events of particle hops. Hops are defined as the successive motions of a sediment particle measured from its start (entrainment) to stop (deposition). The corresponding times spent during the hops are termed as travel times (τ). For comparison, and validation of our analytical solutions in this study, we used the experimental data presented in Fathel *et al.* (2015), which rely on the experimental measurements of Roseberry *et al.* (2012). We note that, based on this specific experimental dataset, our approach is relevant for bedload transport under conditions of low transport rates. However, the theoretical findings of this work may have broader implications, e.g. on the scaling relations for particle motions (see also Wu *et al.* 2020), which requires further evaluation with different experimental datasets in the future.

2.1. *Random walk for particles' velocity variation* Δu

We are interested in understanding how a bedload particle's velocity can change with time during a hop. In figure 1 we display an example of the velocity trajectory during the hop of a single bedload particle, which is randomly selected from the high-resolution experimental measurements of Fathel *et al.* (2015). At first glance, it is reasonable to speculate that the particle's velocity could be described by a random walk process during the hop:

$$\Delta u = u(t + \Delta t) - u(t) = R\sqrt{2D^*\Delta t}, \tag{2.1}$$

where u is the particle's velocity (m s^{-1}), t is time (s), Δu is the change in velocity over an observed time step Δt (in this case an experimental sampling time step as seen in figure 1), D^* is a constant diffusion coefficient (m^2 s^{-3}) and R is a random variable with zero mean and unit variance. Note that the requirement of unit variance for R here is in accordance with that of a finite second-order moment for the distribution of Δu, which guarantees that the random walk process (2.1) will asymptotically approach a diffusion process.

It is easy to check, by putting together all the records of velocity variations Δu obtained by taking the difference between successive particle velocities for the observed trajectories, that these fluctuations have zero mean. In addition, the p.d.f.s of Δu based on different sample sizes can be approximated by a stationary distribution, which ensures the unit variance for R and a constant diffusion coefficient D^* (not shown here).

In the case when the random variable R follows a Gaussian distribution (on top of zero mean and unit variance as stated above), (2.1) would describe a Gaussian random walk process. This would be particularly interesting because one could immediately infer the form of the governing equation for the particle's velocity variations, since the Gaussian

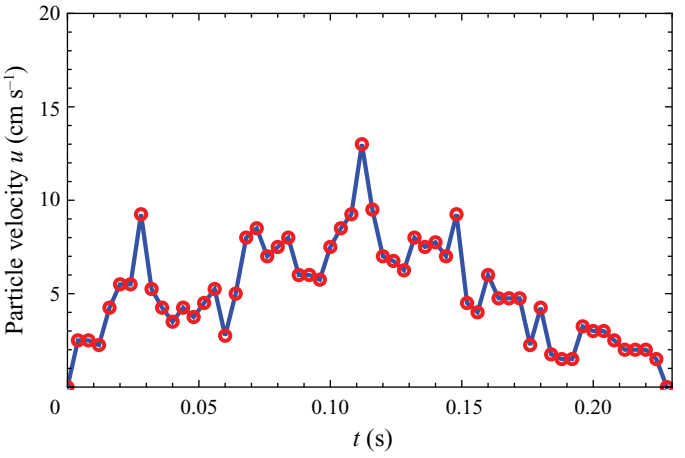

Figure 1. An example of velocity trajectory during the hop of a single bedload particle, which is randomly selected from the high-resolution experimental measurements (Fathel *et al.* 2015).

random walk is equivalent to a diffusion equation (e.g. see Li *et al.* 2017). Accordingly, (2.1) leads to

$$\frac{\partial P_N(u,t)}{\partial t} = D^* \frac{\partial^2 P_N}{\partial u^2}, \tag{2.2}$$

where P_N is the p.d.f. of the particle's velocity under the above assumptions. Note that the form of the distribution for the random variable R can be obtained from the acceleration data, which is calculated from $\Delta u/\Delta t$ (which gives the left-hand side of (2.1) and thus specifies the distribution of R on the right-hand side of (2.1)).

However, experimental results have already rejected the hypothesis of a Gaussian p.d.f. for R, by showing that the acceleration p.d.f. of particle motions is Laplace-like or double-exponential-like (Fathel *et al.* 2015; Liu *et al.* 2019). In figure 2, we provide the calculated statistics of particle velocity variations for the experimentally measured hops. It is obvious from figure 2(*a*) that the p.d.f. of the velocity variations can be well approximated by a Laplace distribution. Figure 2(*b*) presents a quantile–quantile (QQ) plot to quantify how the distribution of Δu deviates from a normal distribution. Notice that in figure 2 we have scaled the velocity variation Δu by a characteristic maximum velocity $u_0 = U_{max}$. We now infer that the velocity variations of bedload particle hops measured along the u-axis may possibly follow a random walk, but not a Gaussian random walk process.

2.2. *Gaussian random walk for the transformed velocity variation* $\Delta\zeta$

Since the p.d.f. of measured velocity variations does not support a diffusion process describing the variation of particle velocity u as shown in (2.2), we hypothesize and rigorously test that a nonlinear transformation exists for mapping the velocity u into a different, scaled velocity $\zeta \in [0, 1]$,

$$u \to \zeta, \tag{2.3}$$

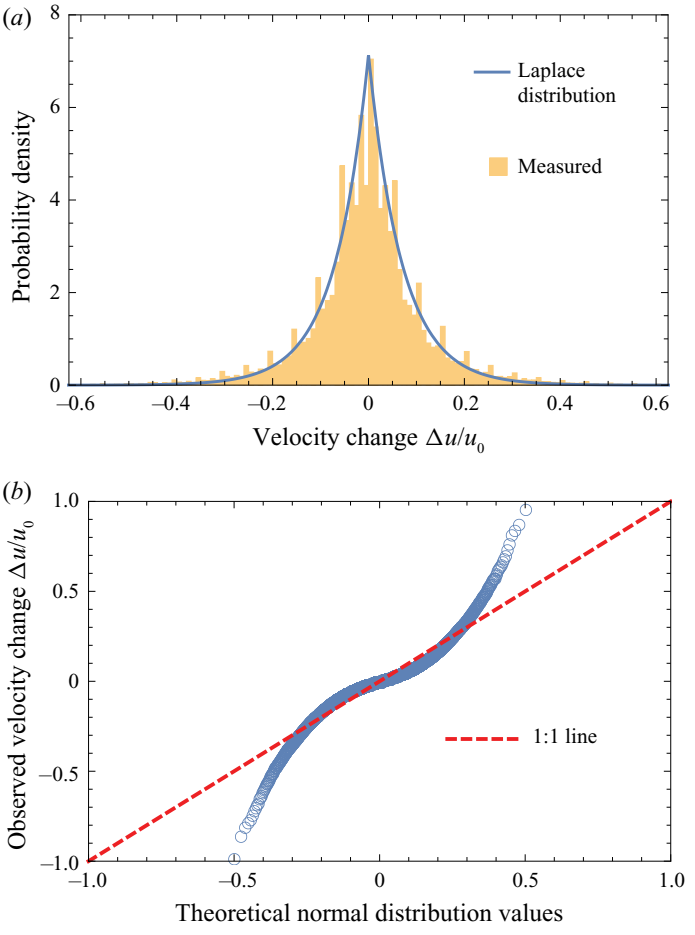

Figure 2. Bedload particle velocity variation statistics for the experimentally measured hops (Fathel *et al.* 2015). (*a*) The p.d.f. of the experimentally measured velocity variations. Notice that we have scaled the velocity variation Δu by a characteristic maximum velocity $u_0 = U_{max}$. (*b*) QQ plot illustrates the deviation of the measured p.d.f. of velocity variation Δu from a normal distribution, suggesting a non-Gaussian distribution for the random variable R in (2.1).

with respect to which the variation of velocity can be governed by a diffusion process:

$$\frac{\partial P_N(\zeta, t)}{\partial t} = D\frac{\partial^2 P_N}{\partial \zeta^2}, \tag{2.4}$$

where D is the corresponding diffusion coefficient (s^{-1}) and the transformed velocity ζ is dimensionless. Qualitatively, as sketched by figure 3, this envisioned transformation nonlinearly maps the velocity u-axis into a ζ-axis in such a way that, for example, the part of the axis close to $u = 0$ is stretched and the part close to $u = U_{max}$ is compressed. Hence, the velocity u in the resulting ζ-axis increases nonlinearly (as ζ increases from 0 to 1), slower in the vicinity of $\zeta = 0$ but faster when it gets close to $\zeta = 1$.

We can then transform (2.4) back with respect to the u-axis:

$$\frac{\partial P_N(u, t)}{\partial t} = DA^2\frac{\partial^2 P_N}{\partial u^2} + DA\frac{\partial A}{\partial u}\frac{\partial P_N}{\partial u}, \tag{2.5}$$

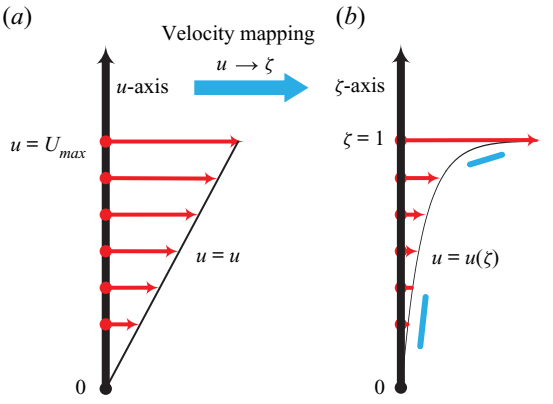

Figure 3. Schematic representation of the nonlinear transformation that maps the velocity u to a scaled velocity ζ. (*a*) The velocity increases linearly as u increases from 0 to U_{max} in the u-axis. (*b*) After the transformation, the velocity increases in a nonlinear manner as ζ increase from 0 to 1: slower when ζ is closer to 0 while faster when ζ is closer to 1.

where

$$A = \frac{\partial u}{\partial \zeta} \tag{2.6}$$

is the mathematical definition of the transformation (2.3), which is a centrepiece of our approach giving the mapping rule for velocity from u to ζ:

$$\zeta(u) = \int_0^u \frac{1}{A}\,\mathrm{d}u. \tag{2.7}$$

Note that the specific form of the proposed nonlinear transformation, which is not known *a priori*, is represented by an explicit expression of the key function A, or the mapping rule $\zeta(u)$. In order to find out the key function A in (2.6) and (2.7), we compare (2.5) to the Fokker–Planck equation, which has recently been shown to be able to describe statistically the transport process of an ensemble of bedload particles (Furbish, Roseberry & Schmeeckle 2012*b*):

$$\frac{\partial P_N(u,t)}{\partial t} = -\frac{\partial}{\partial u}[\mu(u)P_N] + \frac{\partial^2}{\partial u^2}[k(u)P_N]. \tag{2.8}$$

In the above equation μ (m s^{-2}) and k (m^2 s^{-3}) are, respectively, known as the 'drift velocity' and the 'diffusivity' with respect to the velocity u. We expand and rewrite (2.8) in the following form:

$$\begin{aligned}\frac{\partial P_N(u,t)}{\partial t} = k\frac{\partial^2 P_N}{\partial u^2} + c_1\mu\frac{\partial P_N}{\partial u} - \left[\frac{\partial \mu}{\partial u}P_N + (1+c_1)\mu\frac{\partial P_N}{\partial u}\right] \\ + \left(\frac{\partial^2 k}{\partial u^2}P_N + 2\frac{\partial k}{\partial u}\frac{\partial P_N}{\partial u}\right),\end{aligned} \tag{2.9}$$

where c_1 is a constant.

For the equilibrium transport condition, the velocity p.d.f. does not change with time, under which circumstance (2.5) and (2.9) become

$$0 = DA^2 \frac{\partial^2 f_p}{\partial u^2} + DA \frac{\partial A}{\partial u} \frac{\partial f_p}{\partial u}, \tag{2.10a}$$

$$0 = k \frac{\partial^2 f_p}{\partial u^2} + c_1 \mu \frac{\partial f_p}{\partial u} - \left[\frac{\partial \mu}{\partial u} f_p + (1 + c_1) \mu \frac{\partial f_p}{\partial u} \right] + \left(\frac{\partial^2 k}{\partial u^2} f_p + 2 \frac{\partial k}{\partial u} \frac{\partial f_p}{\partial u} \right), \tag{2.10b}$$

where f_p is the temporally stationary p.d.f. of the particle velocity (i.e. the p.d.f. $f_p(u)$ does not change with time).

One possible set of relations for both equations in (2.10) describing the same process can be written as follows:

$$k = DA^2, \tag{2.11a}$$

$$c_1 \mu = DA \frac{\partial A}{\partial u}, \tag{2.11b}$$

$$\frac{\partial \mu}{\partial u} f_p + (1 + c_1) \mu \frac{\partial f_p}{\partial u} = 0, \tag{2.11c}$$

$$\frac{\partial^2 k}{\partial u^2} f_p + 2 \frac{\partial k}{\partial u} \frac{\partial f_p}{\partial u} = 0. \tag{2.11d}$$

This set of equations can be solved to give

$$c_1 = 1, \quad k = \int \frac{c_2}{{f_p}^2} \, \mathrm{d}u, \quad \mu = \frac{c_2}{2{f_p}^2}, \tag{2.12a–c}$$

and the important result

$$A^2 = \frac{c_2}{D} \int f_p^{-2} \, \mathrm{d}u, \tag{2.13}$$

relating the key function A to the temporally stationary particle velocity p.d.f. f_p, which is in accordance with the equilibrium transport conditions as assumed in previous studies (Fathel *et al.* 2015; Liu *et al.* 2019).

We take advantage of recent experimental measurements (Lajeunesse *et al.* 2010; Roseberry *et al.* 2012; Fathel *et al.* 2015) and theoretical analyses (Furbish & Schmeeckle 2013; Fan *et al.* 2014) that have documented an exponential-like form for the particle velocity p.d.f. $f_p(u)$. Hence, we assume that the velocity p.d.f. follows an exponential distribution

$$f_p(u) = \frac{1}{U} \exp\left(-\frac{u}{U}\right), \tag{2.14}$$

where U is the mean velocity. A value U_{max} for the velocity maximum can be adopted in accordance with the near-bed flow velocity, representing a physical constraint on the maximum particle velocity. As demonstrated by Wu *et al.* (2020), U_{max} can be set as 30 cm s^{-1} for the dataset of Fathel *et al.* (2015), and the particle hop processes are not sensitive to this value.

Substituting (2.14) into (2.13), we obtain an explicit expression for the function A:

$$A = \sqrt{\frac{c_2}{D}\int {f_p}^{-2}\,\mathrm{d}u} = \mathrm{e}^{u/U}\sqrt{\frac{U^3 c_2}{2D}}, \tag{2.15}$$

which can be used to determine the rule for mapping the velocity u into ζ according to (2.7):

$$\zeta(u) = \int_0^u \frac{1}{A}\,\mathrm{d}u = \sqrt{\frac{2D}{Uc_2}}\left(1 - \mathrm{e}^{-u/U}\right). \tag{2.16}$$

Recall that we define ζ as a scaled quantity in the range of [0, 1], meaning that

$$\zeta(u)|_{u=0} = 0, \quad \text{and} \quad \zeta(u)|_{u=\infty} = 1. \tag{2.17a,b}$$

The former part of (2.17*a*,*b*) is automatically satisfied according to (2.16), while the latter implies that

$$\sqrt{\frac{2D}{Uc_2}} = 1, \tag{2.18}$$

further simplifying (2.16) to

$$\zeta(u) = 1 - \mathrm{e}^{-u/U}. \tag{2.19}$$

With the above obtained explicit expression for the velocity transformation, we can verify the hypothesis posed at the beginning of this subsection, i.e. a nonlinear transformation exists for the mapped velocity variations governed by a diffusion equation. Specifically, we mapped the experimentally measured particle velocity series into the ζ-axis system according to (2.19), which were then used to calculate the transformed particle velocity variations $\Delta\zeta$ by taking the difference between successive velocities in the ζ-axis. We illustrate in figure 4 that, as opposed to the results expressed in the u-axis (figure 2*b*), the transformed velocity variation $\Delta\zeta$ can be relatively well approximated by a Gaussian distribution, verifying our hypothesis of modelling the velocity variation with respect to the ζ-axis by the diffusion equation (2.4).

In figure 5 we display the p.d.f. of the measured velocity variation expressed in the ζ-axis. The Gaussian distribution reproducing the measurements, with fitted parameters of zero mean and standard deviation $\sigma \approx 0.18$, is superimposed in the figure. This allows us to determine the diffusion coefficient in (2.4) by

$$\sigma^2 = 2D\Delta t, \tag{2.20}$$

which gives

$$D = 4\ \mathrm{s}^{-1} \tag{2.21}$$

based on the time step of experimental measurements of Δt = 1/250 s (the standard deviation is dimensionless, the same as the scaled velocity ζ). Note that we determined the parameter D using the transformed acceleration data (with respect to ζ); however, D can be alternatively estimated with measured hop distances and travel times, as we will demonstrate later in § 3.2.

From a Lagrangian perspective, (2.4) describes how the velocity of the particle changes with time (i.e. follows the Gaussian random walk with respect to ζ), while the streamwise

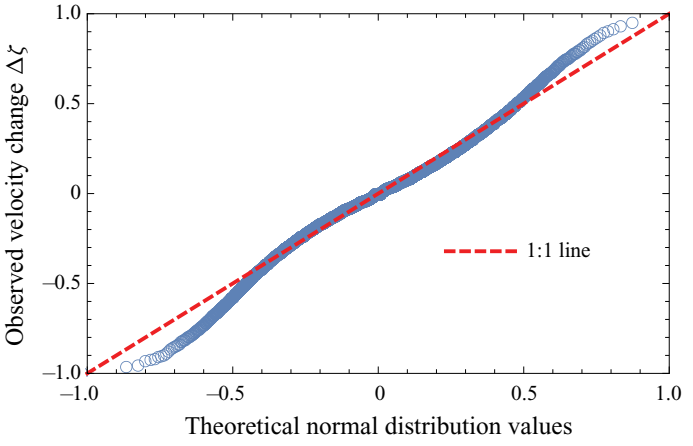

Figure 4. QQ plot illustrates how close the p.d.f. of transformed velocity variation $\Delta\zeta$ can be described by a normal distribution. Compared with results in figure 2(*b*), a normal distribution fits much better to $\Delta\zeta$ instead of Δu. This verifies our hypothesis that a nonlinear transformation exists for modelling the velocity variation with respect to the ζ-axis by a diffusion equation, i.e. (2.4).

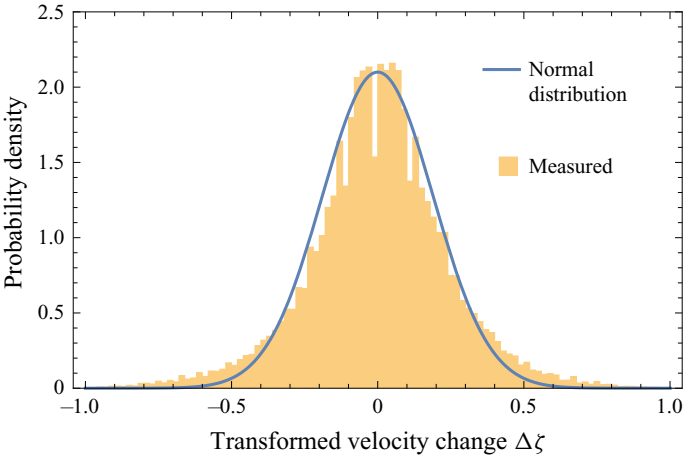

Figure 5. Empirical p.d.f. of transformed velocity variation $\Delta\zeta$ and the fitted normal distribution. The fitted theoretical distribution in the figure has a zero mean and a standard deviation of $\sigma \approx 0.18$.

position of the particle is controlled by the corresponding velocity variations, which can simply be expressed by the following stochastic differential equation:

$$\mathrm{d}x = u(\zeta)\,\mathrm{d}t, \tag{2.22}$$

where x (m) is the streamwise position of the particle. To map the transformed velocity ζ back into u, we only need to solve the inverse function of (2.19):

$$u(\zeta) = -U\log(1-\zeta). \tag{2.23}$$

Notice that (2.4) and (2.22) describe a non-stop transport process for the bedload particle (i.e. the particle is travelling with velocity variations and does not stop). This point is

straightforward if we write down the discrete forms of (2.4) and (2.22), respectively, as

$$\zeta(t+\Delta t) = \zeta(t) + R\sqrt{2D\Delta t}, \tag{2.24a}$$

$$x(t+\Delta t) = x(t) - U\log(1-\zeta)\Delta t, \tag{2.24b}$$

the form of which is commonly used in numerically simulating motions of a single particle in the Lagrangian perspective (i.e. Monte Carlo simulation). In (2.24) the time step Δt needs to be small enough, R is a normally distributed random variable with unit variance, and the overall number of runs of the simulation needs to be large enough. Each run of the simulation provides the trajectory of a single particle, and the ensemble of runs provides statistical information on the motions of bedload particles. It is seen that, without specifying a condition for the cessation of the particle motion for (2.24), a simulated particle is always travelling and does not stop, which we refer to as a 'non-stop transport process'.

The Lagrangian form of (2.24) is more intuitive in describing the physical process of bedload particle transport. However, for convenience in obtaining analytical solutions, we can switch back to the Eulerian description for (2.24), which turns out to be (Dimou 1989; Ancey & Heyman 2014; Li *et al.* 2017)

$$\frac{\partial P_N(x,\zeta,t)}{\partial t} = U\log(1-\zeta)\frac{\partial P_N}{\partial x} + D\frac{\partial^2 P_N}{\partial \zeta^2}, \tag{2.25}$$

where $P_N(x,\zeta,t)$ is now the joint p.d.f. of the streamwise position x, the velocity (with respect to ζ) and the time t. The subscript N further stands for the non-stop process.

Obtaining $\langle P_N\rangle$ with respect to ζ gives the joint p.d.f. of streamwise position and time, where the angle brackets are defined as

$$\langle\,\cdot\,\rangle = \int_0^1 (\,\cdot\,)\,\mathrm{d}\zeta. \tag{2.26}$$

2.3. *Description of the bedload particle hops by the obtained governing equation*

As noted above, without additional constraints, (2.25) represents a non-stop process (the particle never stops its motion during the transport). However, particles move through a sequence of hops during which they must start and stop their motions with zero velocity. To perform a hop, a particle first starts its motion from a stationary position, which can be used to set the initial condition for (2.25) as

$$P|_{t=0} = \delta(x)\delta(\zeta-\zeta_0), \tag{2.27}$$

where $\delta(\,\cdot\,)$ is the Dirac delta function. In this section (§ 2.3), we are imposing constraints aimed at connecting the previously discussed non-stop transport process to the particle hop. To distinguish between the two processes, hereafter we use the notation of $P(x,\zeta,t)$ for the particle hop that is delimited by two resting periods, compared with that of $P_N(x,\zeta,t)$ for the non-stop process.

Equation (2.27) implies that we ignore when and where particles are performing these hops (Wu *et al.* 2020), under which circumstance we can virtually move the starting position of all hops to the same place and allow particles to move at the same time. Specifically, (2.27) states that particles start to move at the time $t=0$, from the streamwise location $x=0$, and with a velocity of $u=u(\zeta_0)$; additionally, applying $\zeta_0\to 0$ gives

the initial velocity of $u = 0$, defining the transition between rest and motion regimes, consistent with the phenomenology of particle hops during the entrainment phase.

During travelling, particles' velocities are confined between the minimum and maximum values:

$$\left.\frac{\partial P}{\partial \zeta}\right|_{\zeta=0} = \left.\frac{\partial P}{\partial \zeta}\right|_{\zeta=1} = 0. \tag{2.28}$$

A moving particle must stop its motion to complete a hop. Experimental studies have suggested that the time for a bedload particle to remain in motion (i.e. the travel time τ) follows an exponential distribution (Martin *et al.* 2012; Roseberry *et al.* 2012; Fathel *et al.* 2015; Liu *et al.* 2019), implying a memoryless process for the termination of the particle hop (Martin *et al.* 2012). To incorporate such a memoryless process into the governing equation, we can add a sink term with the particle deposition rate k_a (s^{-1}) for the non-stop transport process (2.25):

$$\frac{\partial P(x, \zeta, t)}{\partial t} = U \log(1-\zeta)\frac{\partial P}{\partial x} + D\frac{\partial^2 P}{\partial \zeta^2} - k_a P. \tag{2.29}$$

Again, we note that we have dropped the subscript N and use $P(x, \zeta, t)$ for particle hops as first introduced in (2.27). The sink term in (2.29) indicates that the cessation of a particle's motion (thus completing the hop) is an independent, random event, resulting in an exponential distribution for the travel times (Zeng & Chen 2011).

It is easy to perform numerical simulations to extract particle hops using (2.24), based on the above discussed constraints. However, from an Eulerian perspective, we note that the solution of (2.29), $P(x, \zeta, t)$, does not directly correspond to the hop events. We emphasize the fact that $P(x, \zeta, t)$ describes the spatial–temporal (and velocity) evolution for the *active particles*. Such particles have started from zero velocity by considering the initial condition (2.27) but have not yet stopped their motions; because, once they stop, they will no longer be represented by P. Thus, the deduced mean travel distance $L(t)$ based on $P(x, \zeta, t)$ does not represent the mean hop distance of particles (denoted as $L_h(\tau)$ and conditional on particles that have ceased their motions at the time τ), since these particles are still moving and have not stopped at time t.

In order to bridge the gap between the two processes so as to use the solution of (2.29) to obtain the mean hop distance–travel time relation (L_h–τ), we consider an in-between time t_0 during a particle hop ($0 \leq t_0 \leq \tau$), as sketched in figure 6(*a*). Consequently, the mean distance travelled by the active particles $L(t_0)$ can be obtained as the solution of (2.29) with respect to t_0. A further relation between t_0 and τ, and between $L(t_0)$ and $L_h(\tau)$, may enable us to 'translate (or extend)' the result of $L(t_0)$ to obtain $L_h(\tau)$.

Motivated by the intuitive understanding of 'symmetry' for the trajectory of particle hops in an ensemble average sense (i.e. at the initial stage the particle generally accelerates, and before the cessation of motion it generally decelerates), we expect that, for hops with the same travel time: by the 'half travel time' $t_0 = \tau/2$, on average they travel half of the mean hop distance,

$$L_h(\tau) = 2L(t_0)|_{t_0 \equiv \tau/2}. \tag{2.30}$$

We used empirical data to verify the assumption of (2.30). Using the time interval of 0.04 s (i.e. $10\Delta t$) and setting nine successive time intervals of $[0.04(i-1), 0.04i]$ (s), where $i = 1, 2, 3, \ldots, 9$, we divided particle hops into different groups according to their travel times τ. For every group of particle hops, we calculated the mean hop distance $L_h(\tau)$ and the mean travel distance $L(t_0)$ (i.e. found the distance travelled during half of the travel

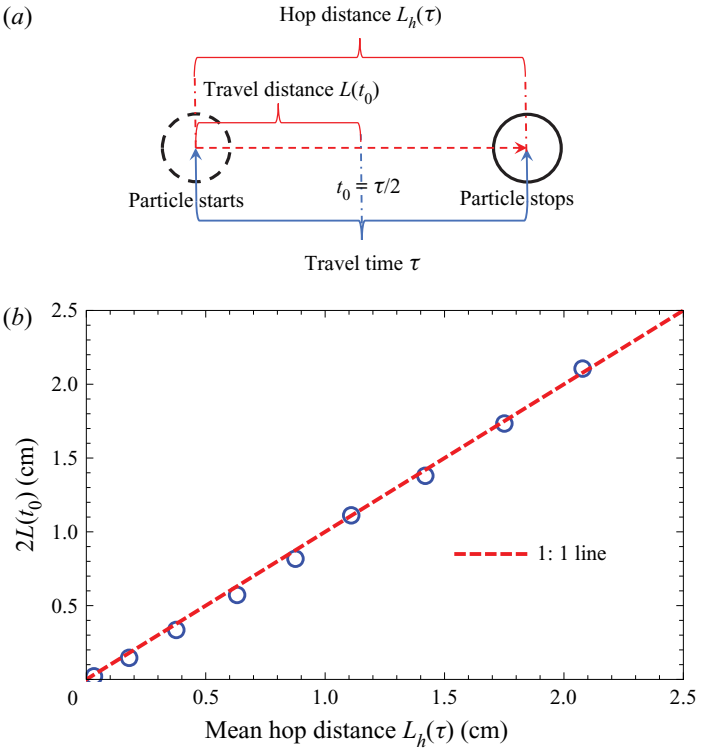

Figure 6. (*a*) Sketch for particle hops with the same travel time τ. Note that the hop/travel distance is an average for an ensemble of particle hops. (*b*)Mean hop/travel distances calculated based on travel times of particle hops for 0.04 s increments, up to 0.36 s. It is seen that the assumption of $L_h(\tau) = 2L(t_0)$ is well supported by empirical data for hops under different travel times, which is critical to 'translate' the solution of (2.29) to obtain the mean hop distance–travel time relation (L_h–τ).

time for every hop, and then calculated the mean over the group of hops). Note that only fewer than 5 % of particle hops travel longer than $10\Delta t = 0.36$ s, too few to guarantee the convergence for the mean hop distances at longer travel-time intervals. Those hops were not included in the analysis. We display the results in figure 6(*b*), demonstrating an excellent support to the assumption of (2.30) for either short or long hops. In § 3 we will analytically solve (2.29) for the mean travel distance $L(t_0)$, and then 'translate' the results based on (2.30) to obtain the mean hop distance–travel time relation (L_h–τ).

3. Results and discussion

We note that the advection–diffusion equation, (2.25), is exactly in the form of the governing equation for a Taylor dispersion process (Taylor 1953), which describes the transport of a solute substance in laminar shear flows. We recall that the flow shear, imposing a spatial difference of streamwise velocities, contributes to the streamwise separation (scattering) of solute molecules (Wu & Chen 2014). The original concept of Taylor dispersion describes the solute molecules performing a Gaussian random walk in a real spatial dimension (e.g. vertically, across the water depth) where they experience different streamwise flow velocities. As a comparison, with (2.25) we envision a virtual velocity dimension ζ for the bedload particle to perform the Gaussian random walk, during

which its streamwise velocity varies by continuously sampling the 'shear flow profile' represented by (2.23). Analytical techniques for studying Taylor dispersion can thus be applied to further analyse the bedload transport process.

3.1. *Analytical solutions*

For the advection–diffusion equation (2.29) with a sink term, it is known that its solution can be expressed as the product of an exponential decay term and the solution of a corresponding non-stop transport process as given by (2.25) (Zeng & Chen 2011):

$$P(x, \zeta, t_0) = P_N(x, \zeta, t_0) \exp(-k_a t_0). \tag{3.1}$$

From a particle-tracking perspective, (3.1) indicates that, while the motion of the particle is governed by a non-stop process (i.e. P_N), the probability for this particle to continue its motion after each time step is determined by an exponential function $\exp(-k_a \Delta t_0)$ until the particle stops.

Based on the knowledge of Taylor dispersion, we understand that (2.25) cannot be analytically solved for P_N, but, instead, that statistical information regarding the bedload particle hops can be obtained through solving the corresponding moment equations (Aris 1956). In fact, (3.1) allows us to define the pth-order moment of $P(x, \zeta, t_0)$ as $M_p(\zeta, t_0)$:

$$M_p(\zeta, t_0) = m_p(\zeta, t_0) \exp(-k_a t_0), \tag{3.2}$$

where

$$m_p(\zeta, t_0) = \int_{-\infty}^{+\infty} P_N(x, \zeta, t_0) x^p \, \mathrm{d}x \tag{3.3}$$

is the pth-order moment for the non-stop bedload transport ($p = 0, 1, 2, \ldots$).

In this work, we consider only the first two statistical moments (i.e. $p = 0$ and 1), which are sufficient for studying the bedload particle hops. As we are going to demonstrate below, the zeroth-order moment $M_0(\zeta, t_0)$ is associated with the travel-time distribution of particle hops; and the first-order moment $M_1(\zeta, t_0)$ specifies the mean hop distance–travel time relation (L_h–τ). Currently, there is only one undetermined parameter (k_a), i.e. the deposition rate in (2.29), which can be fitted to the measured data of travel-time p.d.f. when we solve for the zeroth-order moment $M_0(\zeta, t_0)$. Although the diffusion coefficient D is already obtained in (2.21) by considering the p.d.f. of the transformed velocity variation $\Delta\zeta$, we will demonstrate below how it can be determined alternatively by experimental measurements of travel times and mean hop distances, as a further validation of our theoretical framework.

Applying the operation $\int_{-\infty}^{+\infty}(\,\cdot\,)x^p \, \mathrm{d}x$ to (2.27)–(2.29), we can obtain the zeroth- and first-order moment equations (i.e. $p = 0$ and 1), respectively, as

$$\frac{\partial m_0(\zeta, t_0)}{\partial t_0} = D \frac{\partial^2 m_0}{\partial \zeta^2}, \tag{3.4a}$$

$$\frac{\partial m_1(\zeta, t_0)}{\partial t_0} = D \frac{\partial^2 m_1}{\partial \zeta^2} - U \log(1 - \zeta) m_0(\zeta, t_0), \tag{3.4b}$$

with their initial conditions

$$m_p(\zeta, t_0)|_{t_0=0} = \begin{cases} \delta(\zeta - \zeta_0), & p = 0, \\ 0, & p = 1, \end{cases} \tag{3.5}$$

and corresponding boundary conditions

$$\left.\frac{\partial m_p}{\partial \zeta}\right|_{\zeta=0} = \left.\frac{\partial m_p}{\partial \zeta}\right|_{\zeta=1} = 0. \tag{3.6}$$

Considering $\zeta_0 \to 0$ (bedload particles start their motions with a velocity of $u = 0$), the zeroth-order moment in (3.4) can be solved as

$$m_0(\zeta, t_0) = 1 + 2\sum_{n=1}^{\infty} \cos(\beta_n \zeta) \mathrm{e}^{-D\beta_n^2 t_0}, \tag{3.7}$$

where $\beta_n = n\pi,\ n = 1, 2, 3, \ldots$.

It is obvious that

$$\langle m_0(\zeta, t_0)\rangle = 1 \quad \text{and} \quad \langle M_0(\zeta, t_0)\rangle = \mathrm{e}^{-k_a t_0}, \tag{3.8a,b}$$

indicating that the number of bedload particles in motion remains the same for non-stop bedload transport, but decays exponentially due to deposition which terminates particle hops. Note that $(1 - \langle M_0(\zeta, t_0)\rangle)$ gives the temporal evolution of the probability that the particle has ceased its motion, which is precisely the definition of the cumulative distribution function (c.d.f.) of the travel time for particle hops. Thus, the corresponding p.d.f. can be analytically determined by differentiating it with respect to the time variable t_0:

$$f_T(t_0) = \frac{\mathrm{d}}{\mathrm{d}t_0}(1 - \langle M_0(\zeta, t_0)\rangle) = k_a \mathrm{e}^{-k_a t_0}. \tag{3.9}$$

Recall that t_0 stands for only half of the travel time (i.e. $t_0 = \tau/2$) based on (2.30). When considering the p.d.f. for the entire travel period, (3.9) should be modified as

$$f_T(\tau) = (k_a/2)\mathrm{e}^{-k_a \tau/2}, \tag{3.10}$$

which is an exponential distribution, agreeing with the form observed in experiments (Martin *et al.* 2012; Fathel *et al.* 2015; Liu *et al.* 2019). The mean travel time of the above p.d.f. is $2/k_a$, where the parameter k_a can be determined based on the experimental measurements. For example, Fathel *et al.* (2015) calculated the mean travel time for the particle-tracking experiment as 0.12 s, giving $k_a = 16.67\ \mathrm{s}^{-1}$. Equation (3.10) will be used later to determine the analytical solution for the hop-distance distribution.

We note that the physical meaning of the normalized first-order moment (by the proportion of moving particles, here $\langle M_0\rangle$) is the mean streamwise displacement of bedload particles at a given time, i.e. the mean travel distance of particles with the same half travel time t_0. Thus, $\langle M_1\rangle/\langle M_0\rangle$ eventually gives the mean hop distance–travel time relation (L_h–τ) according to (2.30). Applying the average operator defined in (2.26) on both sides of the first-order moment equation, (3.4*b*), we obtain

$$\frac{\partial \langle m_1\rangle}{\partial t_0} = -U\langle \log(1 - \zeta) m_0(\zeta, t_0)\rangle, \tag{3.11}$$

which can be solved based on the solution of m_0 in (3.7), leading to

$$\begin{aligned} L(t_0) &= \langle M_1\rangle/\langle M_0\rangle = \langle m_1\rangle/\langle m_0\rangle \\ &= Ut_0 + 2U\sum_{n=1}^{\infty} \frac{1 - \mathrm{e}^{-D\beta_n^2 t_0}}{D\beta_n^3} \cos(\beta_n)\mathrm{Si}(\beta_n), \end{aligned} \tag{3.12}$$

where $\mathrm{Si}(\cdot)$ is the sine integral function

$$\mathrm{Si}(\beta_n) = \int_0^{\beta_n} (\sin(z)/z)\,\mathrm{d}z. \tag{3.13}$$

Again, we note that t_0 is only half of the travel time (i.e. $t_0 = \tau/2$); for the entire particle hop, according to (2.30) we have

$$\begin{aligned} L_h(\tau) &= 2L(t_0) = 2L(\tau/2) \\ &= U\tau + 4U\sum_{n=1}^{\infty} \frac{1 - \mathrm{e}^{-D\beta_n^2\tau/2}}{D\beta_n^3} \cos(\beta_n)\mathrm{Si}(\beta_n), \end{aligned} \tag{3.14}$$

which gives the analytical solution for the mean hop distance of an ensemble of particles (L_h) as a function of the travel time (τ).

3.2. *Mean hop distance–travel time scaling for short and long particle hops*

One observation regarding (3.14) is that for long-hop bedload particles ($\tau \to \infty$), the mean hop distance scales linearly with the travel time:

$$L_h(\tau)|_{\tau\to\infty} = U\tau + 4U\sum_{n=1}^{\infty} \frac{\cos(\beta_n)\mathrm{Si}(\beta_n)}{D\beta_n^3} \sim \tau. \tag{3.15}$$

This asymptotic regime was discovered recently (Wu *et al.* 2020) as a correction to previous studies proposing a single regime for the hop-distance scaling (with an exponent of ~ 2 or $\sim 5/3$) of bedload particle motions (Roseberry *et al.* 2012; Fathel *et al.* 2015). The scaling regime of $L_h \sim \tau$ was physically explained by resorting to the earlier formulation by Ancey & Heyman (2014) based on the mean-reverting process, which is valid for the description of long-hop particles (Wu *et al.* 2020). Under the present formulation invoking Taylor dispersion theory, this linear scaling regime is simply known as the Taylor dispersion regime, when the particle has sampled many times possible velocities within the 'shear velocity profile', (2.23). The quote marks represent that it is only mathematically in the same form of the Taylor dispersion process. This understanding indicates that the mean velocity of particle hops converges to a constant U by the time scale $1/D$, where the constant 1 is brought by the normalized velocity ζ. By merely examining the asymptotic regime of the particle hops, i.e. computing the mean velocity of long hops and estimating the starting time of this asymptotic regime, we can roughly estimate the necessary parameters for the governing equation. This point will be further elaborated in later discussion.

As also noted by Wu *et al.* (2020), so far there exists no theory to explain the scaling regime for the short-hop particles, though intuitively it may be attributed to the large proportion of acceleration and deceleration (entrainment and deposition) periods over the entire travel time (of the hop). Owing to the lack of theoretical guidance, and the complicated patterns of short hops, different exponents for the initial scaling regime have been estimated in the literature, and no consensus has been reached for a possibly unified constant. For example, the exponent of 5/3 first appeared in the analysis of a portion of the experimental data by Roseberry *et al.* (2012) (figure 13 in their paper), most of which are now seen for short hops. With much larger datasets used in a reanalysis, Fathel *et al.* (2015) proposed a new exponent of 2 based on a first estimate of the hop distance–travel

time plot (figure 10 in their paper). And this exponent was followed for short hops in the recent study (Wu *et al.* 2020) focusing on scaling regime shifts for particle motions.

While (3.14) does not seem to offer an explicit scaling exponent for the short hops, this analytical solution gives us much more detailed and consistent information compared with numerical simulations (Wu *et al.* 2020). In figure 7(*a*) we present results of (3.14) using three different values of the diffusion coefficient D, respectively, 100, 10 and 1 s^{-1}. The first observation is that different values of D do not affect the long-time asymptotic regime, which agrees with the theoretical expectation of (3.15). However, the time needed for such a transition to the long-time approximation increases as D decreases, which is related to the characteristic time scale $1/D$ by Taylor dispersion theory. Taking the blue curve as an example (for $D = 100\ \mathrm{s}^{-1}$), we can see that one more scaling transition occurred for travel times shorter than $1/D$, as indicated by the two blue solid reference lines with different slopes, which can be used to estimate the scaling exponents as ~ 1.5 and $\sim 5/3$, respectively. We can argue that the time scale of $0.1/D$ sets the upper limit of travel times for the initial regime with the scaling exponent of 1.5. This means that particles have a slow mean velocity when starting the hop, which can increase as $\sim \tau^{0.5}$ if the particle is able to travel longer during a hop. The time scales in between $(0.1/D, 1/D)$ suggest a transition regime. Particle hops with duration falling within the initial and transition regimes can all be defined as short hops, since the mean velocity of these hops has not reached a constant. We note that these scaling regimes could not be identified without the help of the analytical solution of (3.14), given fluctuations and uncertainties observed in numerical and experimental results as shown by figure 4(b) in the paper of Wu *et al.* (2020). The effect of U is more straightforward, as it sets the mean velocity for the long-hop particles (and can thus be determined by the experimental measurements), according to (3.15).

The above discussion provides guidelines for estimating the parameters necessary for particle motions in the governing equation (2.29) using measurements of hop distances and travel times. Based on the experimental data (Fathel *et al.* 2015) for long hops, we can estimate $U = 5.56\ \mathrm{cm\ s}^{-1}$. It can also be observed from the experimental data that the Taylor dispersion regime for particle hops starts approximately between 0.2 and 0.3 s (Wu *et al.* 2020), which gives an estimation of the diffusion coefficient D in the range from 3.33 to 5 s^{-1}. Additionally, fitting (3.14) to measured data of the mean hop distances at different travel times, we can determine the diffusion coefficient D. Note also that our first estimated value of $D = 4\ \mathrm{s}^{-1}$ in (2.21) based on the p.d.f. of the transformed velocity variation $\Delta\zeta$ falls right in the 3.33 to 5 s^{-1} range, corresponding to the average of 0.2 and 0.3 s for $1/D$. The effect of the diffusion coefficient D on the particle motions can be phenomenologically interpreted by considering D as a measure of how fast the particle can change its velocity during the transport. Thus, the faster the particle samples different velocities from the 'shear velocity profile' of (2.23) in a Gaussian random walk manner (measured by the standard deviation of the p.d.f. of $\Delta\zeta$), the shorter time it needs to experience these velocities many times to approach the Taylor dispersion regime for long hops.

In figure 7(*b*), we show that the calculated red points for mean hop distances with respect to travel times from the experimental data are perfectly captured by the solid line representing the analytical solution of (3.14). Since the transition regime for the experimental data starts around $0.1/D = 0.025$ s, it can be seen that an exponent larger than 1.5 (here 5/3) explains quite a portion of the scaling behaviour for the measured short hops (mostly in the transition regime), providing a theoretical basis for the estimation of

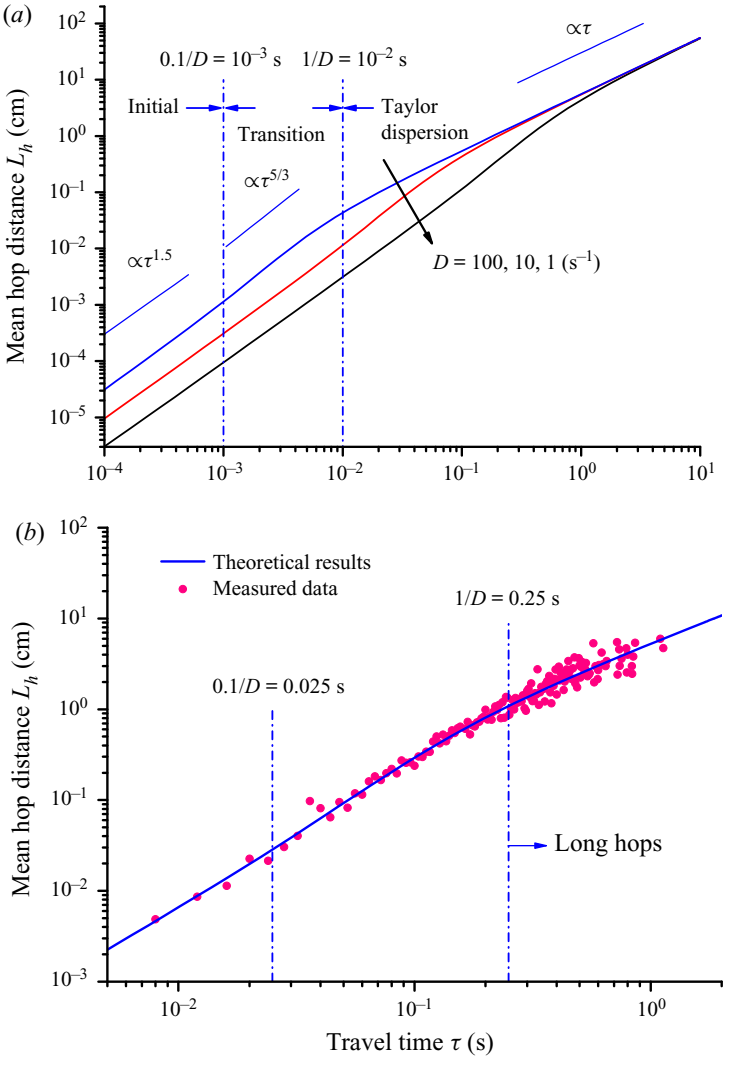

Figure 7. Scaling regimes for mean hop distances (L_h) and travel times (τ) of bedload particle hops. (*a*) Effects of diffusion coefficient D, with two characteristic times of $0.1/D$ and $1/D$ marked for the blue curve of $D = 100\ \mathrm{s}^{-1}$ indicating three stages, respectively, as an initial, a transition and the Taylor dispersion regime. (*b*) Comparison between the experimental data (Fathel *et al.* 2015) for the mean hop distances, which is the same as that presented in figure 4(b) by Wu *et al.* (2020), and the analytical solution (3.14) with parameters of $D = 4\ \mathrm{s}^{-1}$ and $U = 5.56\ \mathrm{cm\ s}^{-1}$.

5/3 made by Roseberry *et al.* (2012). Note also that the present formulation may explain the estimates of lower exponents (in the range 1.25–1.30) as provided from the experiments by Liu *et al.* (2019) in similar transport conditions.

Along with the deposition rate of $k_a = 16.67\ \mathrm{s}^{-1}$ as appeared in equation (3.10), all parameters required in the governing equation (2.29) are now determined. We highlight that, based on the diffusion coefficient $D = 4\ \mathrm{s}^{-1}$ and our demarcation on particles performing short hops (i.e. the travel time $\tau < t_s$, with the characteristic time $t_s = 1/D$), for the Fathel *et al.* (2015) experimental dataset, the number of short hops covers over 84 % of the entire hop events according to the travel-time distribution described by (3.10).

3.3. *Hop-distance distributions*

The hop distance has long been regarded as a key random variable in the formulation of bedload sediment transport, and the form of its distribution is thus of both theoretical and practical importance. Conventionally, the calculation of sediment flux is based on the mean hop distance under equilibrium transport conditions (Einstein 1950), while the second-order moment of the hop-distance distribution comes into play for more generalized cases (Furbish *et al.* 2012*a*). Regarding formulations on bedload tracer transport, where an ensemble of tracer particles is followed during the course of experimental observation, the mean of the hop-distance distribution is necessary for the advective term of the tracer transport, whereas the variance contributes to the streamwise diffusion of tracers (Ganti *et al.* 2010; Wu *et al.* 2019*a*,*b*).

The analytical solution of $L_h(\tau)$ for the mean hop distance–travel time relation allows us not only to distinguish between different transport regimes of particle motions depending on how long the particle can travel during a single hop, but also to straightforwardly and theoretically address the specific form of the hop-distance distribution. Based on the work of Fathel *et al.* (2015) (equation (B1) in their paper) and (3.10) for the travel-time distribution f_T, we have

$$f_L(x) = \left|\frac{\mathrm{d}L^{-1}(x)}{\mathrm{d}x}\right| f_T\left(L^{-1}(x)\right) = \left|\frac{\mathrm{d}L^{-1}(x)}{\mathrm{d}x}\right| \frac{k_a}{2} \exp\left(-\frac{k_a}{2}L^{-1}(x)\right). \tag{3.16}$$

In the above equation, $L^{-1}(x)$ is the inverse function of $L_h(\tau)$, which cannot be given explicitly, but can be calculated numerically according to (3.14). In figure 8 we compare the theoretical result of the hop-distance distribution (3.16) with the experimental measurements, based on the obtained parameters D, U and k_a. The good agreement serves as an excellent validation of the formulation in (2.29) for bedload particle hops. In addition, as also pointed out by Wu *et al.* (2020), the emerging mixed form of the hop-distance distribution, a Weibull-like front and an exponential-like tail, is the result of the different transport regimes for short- and long-hop particles, respectively. That is, the linear scaling of $L_h(\tau) \sim \tau$ for long hops ensures that the tail of the hop-distance p.d.f. is the same as that of the travel times, which is an exponential distribution. And the scaling of $L_h(\tau) \sim \tau^2$ for short hops implies that a different form than the exponential distribution, specifically the Weibull distribution, will emerge for small hop distances in the p.d.f., as concluded by Fathel *et al.* (2015). We note that the tail characteristics of the hop-distance p.d.f. is important in the sense that the heavy-tailed distribution of hop distances was proposed as a possible reason for the observed anomalous diffusion of bedload particle transport (Schumer, Meerschaert & Baeumer 2009). Thus the thin-tailed distribution of hop distances should indicate the existence of different mechanisms leading to the anomalous diffusion, which, for example, can be related to the heavy-tailed waiting time distribution caused by tracer particles when they stop moving and/or get buried (Liu *et al.* 2019; Wu *et al.* 2019*a*,*b*).

In fact, under the current formulation for an exponential distribution of travel times, we can further obtain an explicit expression for the tail of the hop-distance distribution according to the transport regime of the bedload particle performing long hops. Based on the linear relation in (3.15), we have

$$L^{-1}(x)|_{x\to\infty} = \frac{1}{U}x - 4\sum_{n=1}^{\infty} \frac{\cos(\beta_n)\mathrm{Si}(\beta_n)}{D\beta_n^3}, \tag{3.17}$$

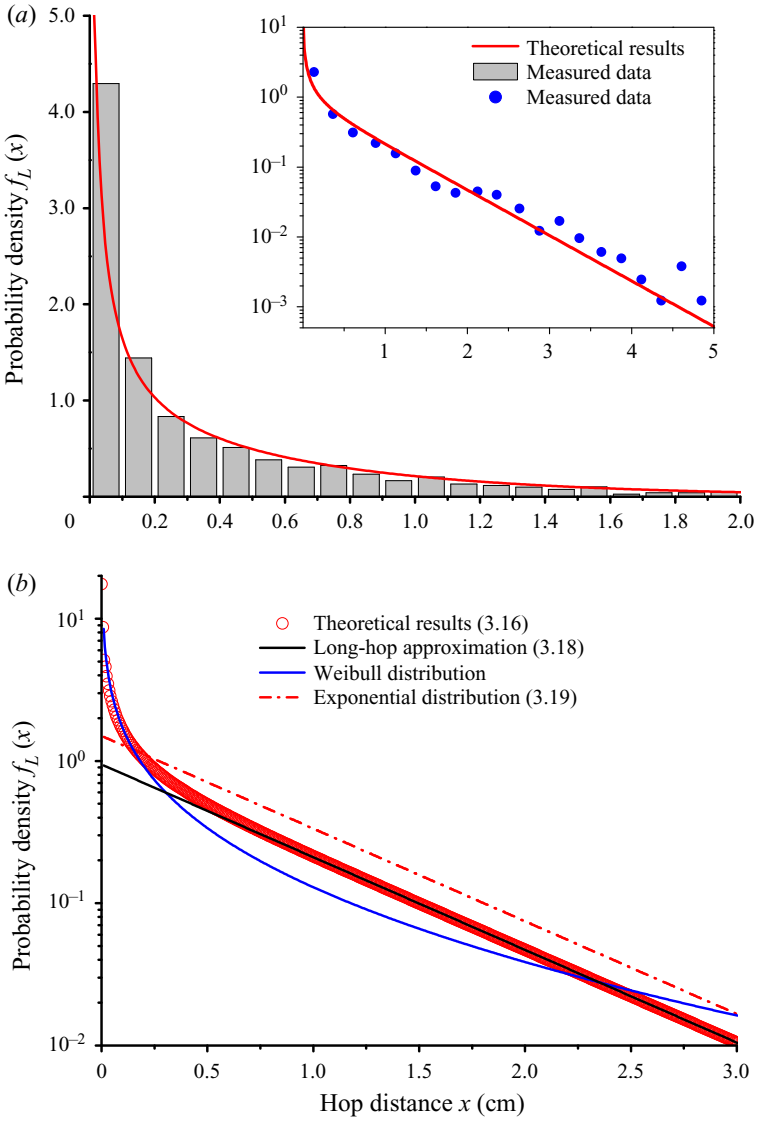

Figure 8. The p.d.f. of bedload particle hop distance. (*a*) Comparison between the experimental data (Fathel *et al.* 2015) and the theoretical result of (3.16). The inset shows the same results presented in linear–log plot. (*b*) Analytical solution for the hop-distance distribution of long hops, in contrast to the Weibull-like front of the distribution for short hops. If there exist only long hops, (3.18) should shift vertically and approach (3.19), which is the exponential p.d.f. for hop-distances conventionally adopted by Einstein (1950) and others in their research.

which results in

$$f_L(x)|_{x\to\infty} = \frac{k_a}{2U}\exp\left(-\frac{k_a}{2U}x + 2k_a\sum_{n=1}^{\infty}\frac{\cos(\beta_n)\mathrm{Si}(\beta_n)}{D\beta_n^3}\right), \tag{3.18}$$

indicating an exponential tail of the distribution, agreeing with our qualitative description. According to (3.16), the linear relation of (3.17) simply tells us that the form of the tail

of the hop-distance distribution must be the same as that of the travel-time distribution (consistent with observations by Roseberry *et al.* 2012; Liu *et al.* 2019).

In figure 8(*b*) we can see that (3.18) captures well the exponential tail of the hop-distance distribution. The Weibull distribution (blue line) in the figure is adopted from Fathel *et al.* (2015): $f_{LW}(x) = \sqrt{x^{-1}/\langle x\rangle/2}\,\exp(-\sqrt{2/\langle x\rangle}\,x^{1/2})$, with the measured mean hop distance $\langle x\rangle = 0.46$ cm. The small differences for short hops between the Weibull distribution and the results of (3.16) are due to different scaling exponents (e.g. 5/3 or 2 for the transition regime) for the mean hop distance–travel time relation. To account for the sharp decay of the probability density by the Weibull-like front due to the large number of particles performing short hops, the black solid line representing (3.18) has to be shifted downwards in the figure as compared with the following exponential p.d.f.:

$$f_{Le}(x) = \frac{k_a}{2U}\exp\left(-\frac{k_a}{2U}x\right). \tag{3.19}$$

Note that (3.19) is only for long hops (i.e. hops with a constant mean velocity), and represents the classic form of hop-distance distribution as assumed by Einstein (1950) and following studies (Paintal 1971; Wu *et al.* 2019*a*).

3.4. *Validation based on the acceleration distribution*

As a further validation of our formulation for the bedload particle hops, we numerically calculated the p.d.f.s of the particle accelerations by particle-tracking simulations based on (2.25). By the algorithm of Gaussian random walk on the ζ-axis (2.24*a*), and the inverse rule for mapping velocity from ζ-axis to u-axis (described by (2.23)), we can generate a time series of velocity u for a particle in motion with the time step of $\Delta t = 0.004$ s, which is the same as the interval used for data sampling in experimental measurements. Note that R in (2.24*a*) is a normally distributed random variable with zero mean and unit standard deviation. The initial and boundary conditions for (2.24*a*) during the simulations are defined by (2.27) and (2.28), respectively. The same parameter of $D = 4\ \mathrm{s}^{-1}$ is used for the simulation. The accelerations are then obtained by $\Delta u/\Delta t$, and the results of our theoretical framework agree well with the measurements by Fathel *et al.* (2015) (figure 9). We note that simulated particle accelerations have not been constrained during the formulation of bedload particle hops in this paper (i.e. (2.29)). Hence, the emerging Laplace form of the acceleration p.d.f. is an independent validation and it is also consistent with recent measurements by Liu *et al.* (2019).

We also note that the Laplace-like p.d.f. for the accelerations in figure 9 is not the result of the exponential-like velocity distribution (as we have assumed in (2.14)). We emphasize that, if the particle velocity is randomly drawn each time from the exponential p.d.f. of (2.14) to construct the velocity trajectory as shown by figure 1, the resulting acceleration p.d.f. is indeed Laplace, but with a different variance compared with the results in figure 9. We have performed such numerical simulations to generate the acceleration p.d.f. as demonstrated in figure 10, which is evidently different from the results in figure 9. This can be attributed to the fact that $\Delta\zeta$ (difference of nonlinearly transformed velocities) in our model is generated by a normally distributed random variable R as seen in (2.24*a*), instead of the difference between two velocities randomly drawn from the exponential p.d.f. of (2.14), respectively.

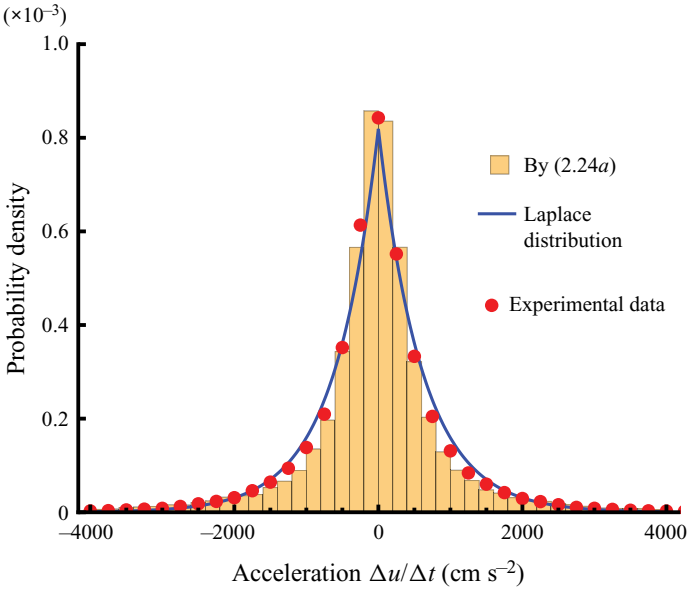

Figure 9. Comparison of acceleration p.d.f.s between the experimental data (Fathel *et al.* 2015) and results of numerical simulation based on the proposed theoretical framework. The Laplace distribution in the figure (blue line) is $f(a_x) = (1/2\lambda)\exp(-|a_x|/\lambda)$, where a_x is the acceleration (cm s^{-2}) and the parameter $\lambda = 610$ cm s^{-2}.

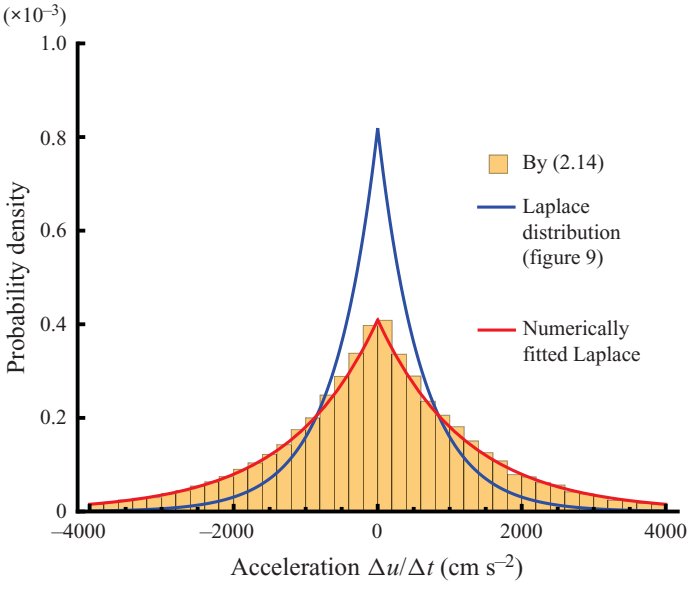

Figure 10. Demonstration that the acceleration p.d.f. in figure 9 is not the result of the exponential distribution of (2.14). The fitted Laplace distribution (red line) to the simulated accelerations in this figure has a very different variance compared to the Laplace p.d.f. in figure 9 (also reproduced here as the blue line). This is because the numerically simulated accelerations were obtained by differences of two velocities each randomly drawn from the exponential distribution of (2.14), rather than that generated by a normally distributed random variable R as seen in (2.24a) and presented in figure 9.

4. Conclusions

In this paper, we investigate the experimental data and find that the velocity variations Δu during particle hops do not follow a Gaussian random walk process. Instead, by performing a nonlinear transformation and mapping the velocity u into an opportunely distorted velocity axis ζ, the corresponding velocity variation $\Delta\zeta$ can be approximated by a Gaussian random walk process, which is equivalent to a governing diffusion equation with respect to the new variable ζ. Using an advection term describing streamwise motions of the particle due to the velocity variations, an advection–diffusion equation is finally deduced for the fundamental events of particle hops, which is seen to be identical with that governing Taylor dispersion. Similar to the Taylor dispersion process describing a solute molecule performing a transverse Gaussian random walk to sample different streamwise flow velocities in a shear flow, in this framework bedload particles perform a Gaussian random walk along a properly transformed velocity ζ. Particles thus sample different velocities from a virtual velocity profile (i.e. (2.23)), which are then translated into their streamwise motion.

Based on the governing equation and the concentration moment method, we obtain the analytical solution for the mean hop distance–travel time relation, which for the first time provides a theoretical basis for the variability of scaling behaviours observed experimentally for particle hops with various travel times and under different transport conditions. The linear hop distance–travel time scaling for long-hop particle motions can simply be explained by the Taylor dispersion regime, with an explicit characteristic time scale t_s $(= 1/D)$ for the mean velocity of the hops to reach a constant value. Travel times shorter than t_s thus define the short hops covering most of the observed particle hops (over 80 % for Fathel *et al.* (2015)), the scaling behaviour of which has not been theoretically explained in previous studies. The solution of our model suggests a slight increase of the scaling exponent from ~ 1.5 at extremely short travel times (initial regime) to $\sim 5/3$ at the beginning of the transition regime, which is characterized by a time scale of $0.1t_s$.

According to Taylor dispersion theory, t_s is closely related to the diffusion coefficient D $(= 1/t_s)$, which characterizes how fast a particle can change its streamwise velocity, and should depend on both flow conditions and particle size, hence on the transport intensity. The prediction of such a key time scale from the transformed velocity variation $\Delta\zeta$ distribution (leading to $t_s = 0.25$ s) agrees well with that observed in experiments ($0.2\ \text{s} < t_s < 0.3$ s). As opposed to using acceleration data, which require high-precision measurements of particle positions, in this paper we demonstrate that the diffusion coefficient D can also be determined by the measured hop distances and travel times, which are more accurate and less experimentally demanding. Future research may provide an opportunity to interpret the diffusion coefficient D using scaling arguments for wall turbulence, for example, as the ratio between the shear velocity and a representative length scale.

Another step forwards is the analytical solution for the p.d.f. of the hop-distance, which is a centrepiece of entrainment formulations for the sediment flux and the Exner equation. Explicit expressions, including that for the tail of the hop-distance distribution, are obtained and used to demonstrate that the conventionally adopted exponential distribution for hop distances, like that proposed by Einstein, is valid solely for long hops (i.e. hops with a constant mean velocity). We simulated the acceleration p.d.f. for particle motions based on the proposed theoretical framework, and compared it with experimental measurements as a further validation of our formulation. The Laplace-like distribution for accelerations is demonstrated not to be the result of the exponential-like velocity distribution of particles.

We acknowledge that the proposed model has been calibrated based on the Fathel *et al.* (2015) dataset. However, we stress that the assumptions of an exponential distribution for streamwise velocity and travel times are robust, as observed in other experimental measurements (Lajeunesse *et al.* 2010; Liu *et al.* 2019). More importantly, the different power-law relations for hop distances and travel times, and the Laplace-like distribution of particle accelerations, are true emerging features of our theoretical framework, in agreement with independent experiments (Fathel *et al.* 2015; Liu *et al.* 2019).

Funding. This work is partially supported by the National Science Foundation of China (51525901) and the National Key Research and Development Programme of China (2016YFE0201900). E.F.-G. acknowledges support by the National Science Foundation (NSF) under grants EAR-1811909, ECCS-1839441 and DMS-1839336. A.S. acknowledges partial support from NSF EAR-1854452.

Declaration of interests. The authors report no conflict of interest.

Author ORCIDs.
Zi Wu https://orcid.org/0000-0003-1231-0893;
Arvind Singh https://orcid.org/0000-0003-2172-6321;
Efi Foufoula-Georgiou https://orcid.org/0000-0003-1078-231X;
Michele Guala https://orcid.org/0000-0002-9788-8119;
Xudong Fu https://orcid.org/0000-0003-0744-0546.

References

Ancey, C. 2010 Stochastic modeling in sediment dynamics: Exner equation for planar bed incipient bed load transport conditions. *J. Geophys. Res.* **115**, F00A11.

Ancey, C., Davison, A., Bohm, T., Jodeau, M. & Frey, P. 2008 Entrainment and motion of coarse particles in a shallow water stream down a steep slope. *J. Fluid Mech.* **595**, 83–114.

Ancey, C. & Heyman, J. 2014 A microstructural approach to bed load transport: mean behaviour and fluctuations of particle transport rates. *J. Fluid Mech.* **744**, 129–168.

Aris, R. 1956 On the dispersion of a solute in a fluid flowing through a tube. *Proc. R. Soc. Lond.* A **235**, 67–77.

Ballio, F., Radice, A., Fathel, S.L. & Furbish, D.J. 2019 Experimental censorship of bed load particle motions, and bias correction of the associated frequency distributions. *J. Geophys. Res.* **124**, 116–136.

Bradley, D.N. 2017 Direct observation of heavy-tailed storage times of bed load tracer particles causing anomalous superdiffusion. *Geophys. Res. Lett.* **44**, 227–235.

Bradley, D.N. & Tucker, G.E. 2012 Measuring gravel transport and dispersion in a mountain river using passive radio tracers. *Earth Surf. Process. Landf.* **37**, 1034–1045.

Campagnol, J., Radice, A., Ballio, F. & Nikora, V. 2015 Particle motion and diffusion at weak bed load: accounting for unsteadiness effects of entrainment and disentrainment. *J. Hydraul. Res.* **53**, 633–648.

Charru, F., Mouilleron, H. & Eiff, O. 2004 Erosion and deposition of particles on a bed sheared by a viscous flow. *J. Fluid Mech.* **519**, 55–80.

Dimou, K. 1989 *Simulation of Estuary Mixing Using a Two-Dimensional Random Walk Model*. Massachusetts Institute of Technology.

Einstein, H. 1937 *Bedload Transport as a Probability Problem. Sedimentation (reprinted in 1972)*, pp. 105–108. Water Resources Publications.

Einstein, H.A. 1950 *The Bed-Load Function for Sediment Transportation in Open Channel Flows*. US Department of Agriculture.

Fan, N., Singh, A., Guala, M., Foufoula-Georgiou, E. & Wu, B. 2016 Exploring a semimechanistic episodic Langevin model for bed load transport: emergence of normal and anomalous advection and diffusion regimes. *Water Resour. Res.* **52**, 2789–2801.

Fan, N., Zhong, D., Wu, B., Foufoula-Georgiou, E. & Guala, M. 2014 A mechanistic-stochastic formulation of bed load particle motions: from individual particle forces to the Fokker-Planck equation under low transport rates. *J. Geophys. Res.* **119**, 464–482.

Fathel, S.L., Furbish, D.J. & Schmeeckle, M.W. 2015 Experimental evidence of statistical ensemble behavior in bed load sediment transport. *J. Geophys. Res.* **120**, 2298–2317.

FURBISH, D.J., HAFF, P.K., ROSEBERRY, J.C. & SCHMEECKLE, M.W. 2012*a* A probabilistic description of the bed load sediment flux: 1. Theory. *J. Geophys. Res.* **117**, F03031.

FURBISH, D.J., ROSEBERRY, J.C. & SCHMEECKLE, M.W. 2012*b* A probabilistic description of the bed load sediment flux: 3. The particle velocity distribution and the diffusive flux. *J. Geophys. Res.* **117**, F03033.

FURBISH, D.J. & SCHMEECKLE, M.W. 2013 A probabilistic derivation of the exponential-like distribution of bed load particle velocities. *Water Resour. Res.* **49**, 1537–1551.

GANTI, V., MEERSCHAERT, M.M., FOUFOULA-GEORGIOU, E., VIPARELLI, E. & PARKER, G. 2010 Normal and anomalous diffusion of gravel tracer particles in rivers. *J. Geophys. Res.* **115**, F00A12.

GONZALEZ, C., RICHTER, D.H., BOLSTER, D., BATEMAN, S., CALANTONI, J. & ESCAURIAZA, C. 2017 Characterization of bedload intermittency near the threshold of motion using a Lagrangian sediment transport model. *Environ. Fluid Mech.* **17**, 111–137.

HASSAN, M.A., CHURCH, M. & SCHICK, A.P. 1991 Distance of movement of coarse particles in gravel bed streams. *Water Resour. Res.* **27**, 503–511.

HASSAN, M.A., VOEPEL, H., SCHUMER, R., PARKER, G. & FRACCAROLLO, L. 2013 Displacement characteristics of coarse fluvial bed sediment. *J. Geophys. Res.* **118**, 155–165.

HOSSEINI-SADABADI, S.A., RADICE, A. & BALLIO, F. 2019 On reasons of the scatter of literature data for bed-load particle hops. *Water Resour. Res.* **55**, 1698–1706.

LAJEUNESSE, E., DEVAUCHELLE, O. & JAMES, F. 2018 Advection and dispersion of bed load tracers. *Earth Surf. Dynam.* **6**, 389–399.

LAJEUNESSE, E., MALVERTI, L. & CHARRU, F. 2010 Bed load transport in turbulent flow at the grain scale: experiments and modeling. *J. Geophys. Res.* **115**, F04001.

LI, A., AUBENEAU, A.F., BOLSTER, D., TANK, J.L. & PACKMAN, A.I. 2017 Covariation in patterns of turbulence-driven hyporheic flow and denitrification enhances reach-scale nitrogen removal. *Water Resour. Res.* **53**, 6927–6944.

LIU, M., PELOSI, A. & GUALA, M. 2019 A statistical description of particle motion and rest regimes in open-channel flows under low bedload transport. *J. Geophys. Res.* **124**, 2666–2688.

MARTIN, R.L., JEROLMACK, D.J. & SCHUMER, R. 2012 The physical basis for anomalous diffusion in bed load transport. *J. Geophys. Res.* **117**, F01018.

PAINTAL, A. 1971 A stochastic model of bed load transport. *J. Hydraul. Res.* **9**, 527–554.

PARKER, G., PAOLA, C. & LECLAIR, S. 2000 Probabilistic Exner sediment continuity equation for mixtures with no active layer. *J. Hydraul. Engng* **126**, 818–826.

PELOSI, A., SCHUMER, R., PARKER, G. & FERGUSON, R. 2016 The cause of advective slowdown of tracer pebbles in rivers: implementation of Exner based master equation for coevolving streamwise and vertical dispersion. *J. Geophys. Res.* **121**, 623–637.

ROSEBERRY, J.C., SCHMEECKLE, M.W. & FURBISH, D.J. 2012 A probabilistic description of the bed load sediment flux: 2. Particle activity and motions. *J. Geophys. Res.* **117**, F03032.

SCHUMER, R., MEERSCHAERT, M.M. & BAEUMER, B. 2009 Fractional advection-dispersion equations for modeling transport at the earth surface. *J. Geophys. Res.* **114**, F00A07.

SEIZILLES, G., LAJEUNESSE, E., DEVAUCHELLE, O. & BAK, M. 2014 Cross-stream diffusion in bedload transport. *Phys. Fluids* **26**, 013302.

TAYLOR, G. 1953 Dispersion of soluble matter in solvent flowing slowly through a tube. *Proc. R. Soc. Lond.* A **219**, 186–203.

WILSON, G.W. 2018 Anomalous diffusion of sand tracer particles under waves. *J. Geophys. Res.* **123**, 3055–3068.

WU, Z. & CHEN, G.Q. 2014 Approach to transverse uniformity of concentration distribution of a solute in a solvent flowing along a straight pipe. *J. Fluid Mech.* **740**, 196–213.

WU, Z., FOUFOULA-GEORGIOU, E., PARKER, G., SINGH, A., FU, X. & WANG, G. 2019*a* Analytical solution for anomalous diffusion of bedload tracers gradually undergoing burial. *J. Geophys. Res.* **124**, 21–37.

WU, Z., FURBISH, D. & FOUFOULA-GEORGIOU, E. 2020 Generalization of hop distance-time scaling and particle velocity distributions via a two-regime formalism of bedload particle motions. *Water Resour. Res.* **56**, e2019WR025116.

WU, Z., SINGH, A., FU, X. & WANG, G. 2019*b* Transient anomalous diffusion and advective slowdown of bedload tracers by particle burial and exhumation. *Water Resour. Res.* **55**, 7964–7982.

YAGER, E., KENWORTHY, M. & MONSALVE, A. 2015 Taking the river inside: fundamental advances from laboratory experiments in measuring and understanding bedload transport processes. *Geomorphology* **244**, 21–32.

ZENG, L. & CHEN, G.Q. 2011 Ecological degradation and hydraulic dispersion of contaminant in wetland. *Ecol. Model.* **222**, 293–300.